



## ATF3 expression in cardiomyocytes and myofibroblasts following transverse aortic constriction displays distinct phenotypes



Abu-Sharki Soraya<sup>a,1</sup>, Haas Tali<sup>b,1</sup>, Shofti Rona<sup>b</sup>, Friedman Tom<sup>a,c</sup>, Kalfon Roy<sup>a</sup>, Aronheim Ami<sup>a,\*</sup>

<sup>a</sup> Department of Cell Biology and Cancer Science, The Ruth and Bruce Rappaport, Faculty of Medicine, Technion – Israel Institute of Technology, Haifa, Israel

<sup>b</sup> The Pre-Clinical Research Authority Unit, Technion – Israel Institute of Technology, Haifa, Israel

<sup>c</sup> Department of Cardiac Surgery, Rambam Medical Center, Haifa, Israel

### ARTICLE INFO

#### Article history:

Received 26 August 2020

Received in revised form 10 December 2020

Accepted 12 December 2020

#### Keywords:

Cardiac remodeling

Hypertrophy

Heart failure

Pressure overload

Cardiomyocytes fibroblasts

Conditional knockout

### ABSTRACT

**Background:** Activating transcription 3 (ATF3) is a member of the basic leucine zipper family of transcription factors. ATF3 is an immediate early gene expressed following various cellular stresses. ATF3 acts through binding to cyclic AMP response elements found in the promoters of key regulatory proteins that determine cell fate. In the heart, multiple cardiac stresses result in chronic ATF3 expression. Transgenic mice with ATF3 expression in cardiomyocytes clearly demonstrate that ATF3 serves a leading role in heart hypertrophy, cardiac fibrosis, cardiac dysfunction and death. In contrast, the use of ATF3 whole body knockout mice resulted non-conclusive results. The heart is composed of various cell types such as cardiomyocytes, fibroblasts, endothelial and immune cells. The question that we addressed in this study is whether ablation of ATF3 in unique cell types in the heart results in diverse cardiac phenotypes. **Methods:** ATF3-flox mice were crossed with  $\alpha$ MHC and Postn specific promoters directing CRE expression and thus ATF3 ablation in cardiomyocytes and myofibroblast cells. Mice were challenged with transverse aortic constriction (TAC) for eight weeks and heart function, ventricle weight, hypertrophic markers, fibrosis markers and ATF3 expression were assessed by qRT-PCR.

**Results:** The results of the study show that ATF3 deletion in cardiomyocytes followed by TAC resulted in reduced heart growth and dampened fibrosis response while ATF3 ablation in myofibroblasts displayed a reduced hypertrophic gene program.

**Conclusions:** TAC-operation results in increased ATF3 expression in both myofibroblasts and cardiomyocytes that promotes a hypertrophic program and fibrotic cardiac growth, respectively.

© 2020 The Authors. Published by Elsevier B.V. This is an open access article under the CC BY-NC-ND license (<http://creativecommons.org/licenses/by-nc-nd/4.0/>).

## 1. Introduction

Cardiac remodeling in the heart is a response to physiological, pathological and pharmacological stresses [1,2]. Cardiac remodeling is an adaptive process that preserves efficient heart function in response to different conditions to provide sufficient blood supply. These adaptive changes are transient and reversible [3]. Nevertheless, once the stress becomes chronic, the adaptive changes becomes maladaptive and irreversible leading to fibrosis, reduced contractile function, heart failure and death [4]. Cardiac remodeling is specified by an altered gene expression program induced by a large number of transcription factors that coordinate the cardiac response to changes to multiple environmental cues [5]. A

case in point is ATF3, a transcription factor and member of the bZIP super family [6]. ATF3 is expressed at very low levels under normal conditions, but its expression is highly elevated following various cardiac stresses [6]. In addition, high ATF3 expression levels were found in patients with heart failure [7]. Numerous studies from our group and others have provided compelling evidence consistent with a maladaptive role for ATF3 expression in the heart. First, during development stages, ATF3 expression in cardiomyocytes results in enlarged atria with conduction defect and sudden death [8,9]. Second, in adults, ATF3 expression in cardiomyocytes resulted in hypertrophy, fibrosis, cardiac dysfunction and early death [9]. Third, mice lacking ATF3 expression displayed reduced cardiac remodeling following exposure to chronic high blood pressure [10,11]. In addition, inconsistent results were described for the role of ATF3 expression in the heart after TAC, a pressure overload model in mice. Results from our lab suggest that ATF3 ablation results in a slight protective role [12] while another study described a worsened phenotype in mice lacking ATF3 following

\* Corresponding author at: 7th Efron St. Bat-Galim, POBOX 9649, Haifa 31096, Israel.

E-mail address: [aronheim@technion.ac.il](mailto:aronheim@technion.ac.il) (A. Ami).

<sup>1</sup> The first two authors contributed equally to this work.

TAC [7]. To further study this discrepancy, we dissected the role of ATF3 expression in either one of the two major cell components in the heart, myofibroblasts and cardiomyocytes. This was done by using ATF3-flox mice crossed with the available transgenic mice directing CRE expression to cardiomyocytes and activated fibroblasts i.e.  $\alpha$ MHC-CRE and Periostin-CRE-ER, respectively. The results suggest that the expression of ATF3 in either type of cell in the heart contributes to a distinct maladaptive response to pressure overload following TAC.

## 2. Material and methods

All experimental protocols were approved by the Institutional Committee for Animal Care and Use at the Technion, Israel Institute of Technology, Faculty of Medicine, Haifa, Israel. All study procedures complied with the Animal Welfare Act of 1966 (P.L. 89–544), as amended by the Animal Welfare Act of 1970 (P.L.91–579) and 1976 (P.L. 94–279).

### 2.1. Animals

All surgeries were performed under isoflurane anesthesia and use of analgesics such as Buprenorphine post-surgery.

The ATF3 gene is located on chromosome 1. Mice with ATF3 flox allele were generated to delete ATF3 specifically in cardiomyocytes using the  $\alpha$ MHC-CRE (Myh6-CRE) [13], and in activated fibroblasts through tamoxifen inducible using Periostin-CRE-ER (Postn-CRE-ER The Jackson Laboratories Stock No: 029645).

Tamoxifen (#T5648-1G, SIGMA) was diluted to 10 mg/mL with corn oil and 10% EtOH. TAC-operated ATF3-flox Postn-CRE-ER and Control ATF3-flox male mice were injected two days post-operation intraperitoneally (IP) with Tamoxifen 40 mg/kg/day for five consecutive days.

### 2.2. Transverse aortic constriction

Transverse aortic constriction (TAC) surgery was performed on 10–12 weeks old male mice with the following genotypes: ATF3<sup>flox/flox</sup>,  $\alpha$ MHC-CRE ATF3<sup>flox/flox</sup> and Postn-CRE-ER, ATF3<sup>flox/flox</sup>. Constriction was performed using a 27G blunt needle to create a standardized constriction of the aorta as was previously described [14]. All TAC procedures in this study were performed by same individual, blinded to the mice genotype.

### 2.3. Magnetic resonance imaging (MRI) acquisition and analysis

Cardiac MRI was performed to measure cardiac function and determine the severity of the TAC surgery. Details of the MRI and all other related experimental methods were described previously [12,15]. EF was calculated as follows:  $EF (\%) = [(LVEDV - LVESV) / LVEDV] \times 100$ .

### 2.4. Echocardiography

Mice were anesthetized with 1% of isoflurane and kept on a 37C heated plate throughout the procedure. An echocardiography was performed using a Vevo2100 micro-ultrasound imaging system (VisualSonics, Fujifilm) which was equipped with 13–38 MHz (MS 400) and 22 55 MHz (MS550D) linear array transducers. Those performing echocardiography and data analysis were blinded to the mice genotype. Cardiac size, shape, and function were analyzed by conventional two-dimensional imaging and M-Mode recordings. Maximal left ventricular end-diastolic (LVDD) and end-systolic (LVDs) dimensions were measured in short-axis M-mode images.

Fractional shortening (FS) was calculated as follows:  $FS (\%) = [(LVDD - LVDs) / LVDD] \times 100$ .

All values were based on the average of at least five measurements.

### 2.5. Heart harvesting

Eight weeks following TAC, mice were anesthetized, weighed and sacrificed. Hearts were excised and weighed and were used for RNA extraction. mRNA was purified from ventricles using an Aurum total RNA fatty or fibrous tissue kit (#732–6830, Bio-Rad) according to the manufacturer’s instructions.

### 2.6. Quantitative real time PCR (qRT-PCR)

cDNA was synthesized from 1000 ng of purified mRNA derived from the ventricles. Purified mRNA was added to a total reaction mix of high-capacity cDNA reverse transcription kit (#4368814, Applied Biosystems) in a final volume of 20  $\mu$ l. Real-time PCR was performed using Rotor-Gene 6000TM (Corbett) equipment with absolute blue SYBR green ROX mix (Thermo Scientific AB-4162/B). Serial dilutions of a standard sample were included for each gene to generate a standard curve. Values were normalized to GAPDH unless otherwise indicated.

Primer name	Primer sequence 5'–3'
<b>GAPDH</b>	F-TTGCCATCAACGACCCCTTCAT R-AGACTCCACGACATACTCAGCA
<b>HSP90</b>	F-TCGTCAGAGCTGATGATGAAGT R-GCGTTAACCATCCAAGTGAAT
<b>ATF3</b>	F-GAGGATTTTGCTAACCTGACACC R-TTGACGGTAAGTACTCCAGC
<b>ANP (atrial natriuretic peptide)</b>	F-GCTTCCAGGCCATATTGGAG R-GGGGGCATGACCTCATCTT
<b>BNP (brain natriuretic peptide)</b>	F-GAGGTCCTCTATCCTCTGG R-GCCATTTCCTCCGACTTTTCTC;
<b>ACTA1 (skeletal actin)</b>	F-GTGAGATTGTGCGCGACATC R-GGCAACGGAAACGCTCATT
<b>Col1<math>\alpha</math></b>	F-CTGGCGGTTTCAGGTCCAAT R-TTCCAGGCAATCCACGAGC
<b>TGF<math>\beta</math></b>	F-CCTGGCCCTGCTGAAGTCTG R-GACGTGGGTCATCACCGAT
<b>CTGF</b>	F-AGACCTGTGGGATGGGCAT R-GCTTGGCGATTTTAGGTGTCC
<b>ACTA2</b>	F-GTCCCAGACATCAGGGAGTAA R-TCGGATACTTCAGCGTCAGGA
<b>Col3<math>\alpha</math>1</b>	F-CTGTAACATGGAAACTGGGGAAA R-CCATAGCTGAACTGAAAACCACC

### 2.7. Statistics

Data is expressed as means  $\pm$  SE. The comparison between several means was analyzed by one-way ANOVA followed by Tukey’s

post hoc analysis. All statistical analyses were performed using GraphPad Prism 5 software (La Jolla, CA). A P value  $\leq 0.05$  was accepted as statistically significant.

### 3. Results

To assess the potential role of ATF3 in the remodeled heart, we used qRT-PCR of mRNA derived from TAC-operated and control C57Bl6 mice. ATF3 expression was significantly induced already eight weeks following TAC (Fig. 1A). The increase in ATF3 transcription is consistent with RNA-sequencing data from hearts harvested from mice sacrificed at different time points after TAC procedure [16]. To explore the role of ATF3 expression in cardiomyocytes of the remodeled heart, we used ATF3-flox mice [ATF3-flox] [17]. Mice were crossed consecutively with  $\alpha$ MHC-CRE transgenic mice [13] (Fig. 1B).  $\alpha$ MHC promoter is constitutively active in cardiomyocytes shortly before birth [18]. Therefore, CRE recombinase is expected to remove the first encoding exon in ATF3 (exon B) in newborn mice [17,19]. These mice were designated ATF3-cardiomyocytes-KO (ATF3-cKO). Similarly to ATF3 whole-body KO mice, ATF3-cKO are viable, fertile and display no overt phenotype. Next, 10–12 weeks old mice were either un-operated or challenged with TAC. ATF3-flox mice lacking CRE served as controls. Eight weeks following TAC, mice were subjected to cardiac MRI, the gold standard for LV function. Non-operated mice from both genotypes displayed no significant difference in ejection fraction (EF) (Fig. 1C). In contrast, TAC-operated mice from both genotypes displayed a significantly lower EF as compared to non-operated mice. No significant difference was observed between TAC-operated mice of both genotypes. Mice were sacrificed 8 weeks following TAC and hearts were harvested and weighed. The hearts from TAC-operated mice displayed a significantly higher ratio of ventricles/body weight (VW/BW) compared to non-operated genotype matched ATF3-flox mice (Fig. 1D). However, ATF3-cKO displayed significantly lower increase in the VW/BW as compared with ATF3-flox control mice after TAC. To verify the efficiency and successful ATF3 ablation, we measured the mRNA levels of ATF3 using quantitative RT-PCR (qRT-PCR). Consistent with Fig. 1A, ATF3 expression remained higher in TAC operated mice even eight weeks following TAC (Fig. 1E). The mice expressing CRE recombinase displayed very low ATF3 expression even lower than the levels observed in naïve mice (Fig. 1E). Demonstrating and validating the use of ATF3-flox / CRE approach to direct ATF3 ablation specifically to cardiomyocytes. Next, we examined the cardiac expression of various hypertrophic markers as an indication of a remodeled heart using qRT-PCR. Following TAC, ATF3-flox mice displayed a significant increase in all three hypertrophic markers ANP, BNP and Acta1 (Fig. 2A). In contrast, in ATF3-cKO mice, only ANP was higher in control un-operated mice. The increase in the basal level of ANP transcription is consistent with our previous results with whole body ATF3-KO [12]. ANP expression was further elevated in TAC-operated ATF3-cKO mice and reached the level of the TAC-operated control mice. In contrast, BNP and Acta1 basal levels were similar in both genotypes. Following TAC, BNP and Acta1 expression levels were elevated in the hearts derived from ATF3-flox mice but failed to do so in the TAC-operated ATF3-cKO (Fig. 2A). We also examined fibrosis hallmark genes by qRT-PCR (Fig. 2B). While there was no difference in the levels of fibrosis markers in non-operated mice, TAC-operated control ATF3-flox mice displayed significantly higher levels in three out of the five markers as compared with ATF3-cKO mice in which none of the markers differed from control un-operated mice. Collectively, mice with ATF3 ablation in cardiomyocytes responded similarly to TAC as compared with their control counterparts except for a significantly lower VW/BW ratio and reduced

fibrosis markers. This result is consistent with our previous study using mice with whole body ATF3-KO in which we observed lower levels of several fibrosis markers [12]. Nevertheless, although fibrosis markers were similar to control, Masson trichrome staining showed lower staining compared to WT that did not reach statistical significance [12]. Therefore, we did not include heart section Masson trichrome staining in this study.

To examine the role of ATF3 expression in cardiac fibroblasts cells, we crossed the ATF3-flox mice with transgenic mice expressing CRE fused to ligand binding domain of the estrogen receptor (CRE-ER) under the control of the Periostin promoter (Fig. 3A) [20]. The CRE-ER fusion protein is located in the cytoplasm in Periostin expressing cells (Myofibroblasts cells) and therefore, in order to obtain CRE-ER translocation to the nucleus, it requires the addition of the estrogen agonist, tamoxifen, provided by IP injections (Fig. 3A). Mice expressing CRE-ER treated with tamoxifen directing ATF3-fibroblasts-KO are designated ATF3-fKO. Similar to ATF3-cKO, ATF3-fKO are viable, fertile and display no overt phenotype. To optimize the timing of tamoxifen injection after TAC operation, we first studied the kinetics of Periostin expression in the heart following TAC using the RNA-sequencing data [16]. This analysis showed that Periostin transcription peaks during the first week following TAC and declines thereafter. Periostin expression remains at about ~5 folds higher compared to sham control four weeks following TAC (Fig. 3B) and about twice as high eight weeks after TAC [21]. Therefore, to induce ATF3-flox ablation soon after TAC, we used five consecutive daily injection of tamoxifen starting two days after TAC-operation. Non-operated ATF3-flox CRE-ER positive mice injected with tamoxifen were used as controls. Eight weeks following TAC, mice were analyzed by echocardiography. TAC-operated ATF3-flox mice lacking CRE were used for comparison with fibroblast ATF3 ablated mice (ATF3-fKO). We first evaluated cardiac function by assessing fractional shortening (FS) from echocardiography analysis. As expected, a reduced FS was observed for both genotypes following TAC with no significant difference between mice genotypes (Fig. 3C). Mice were sacrificed 8 weeks following TAC and hearts were harvested and weighed. The hearts from TAC-operated mice displayed significantly higher VW/BW ratios as compared to ATF3-flox control mice but no difference was observed between the two genotypes (Fig. 3D). To verify the efficiency of successful ATF3 ablation, we measured ATF3 mRNA levels using qRT-PCR and found that following TAC, the CRE expressing mice displayed significant reduced ATF3 expression levels (Fig. 3E), thus demonstrating and validating the conditional KO approach directed specifically to myofibroblasts. We next examined the cardiac expression of various hallmark hypertrophic markers as an indication for heart hypertrophy using qRT-PCR. Whereas control ATF3-flox TAC-operated mice displayed a significant increase in hypertrophic markers ANP, BNP and Acta1 compared to control non-operated mice, ATF3-fKO displayed a dampened hypertrophic response (Fig. 4A). In contrast, following TAC, ATF3-fKO displayed no difference in the expression of all fibrosis hallmark genes tested (Fig. 4B). Collectively, mice with ATF3 ablation directed specifically to myofibroblasts displayed a significantly reduced hypertrophic response following TAC.

### 4. Discussion

The heart is constantly exposed to changing requirements in blood supply. As long as these changes are transient, the adaptive changes are short-lived and reversible [3]. Nevertheless, chronic changes require sustained remodeling which are adaptive at the early stages but becomes maladaptive with time resulting in heart failure and death [5]. Indeed, heart failure remains an unmet need for novel therapeutic interventions [22]. Large numbers of tran-

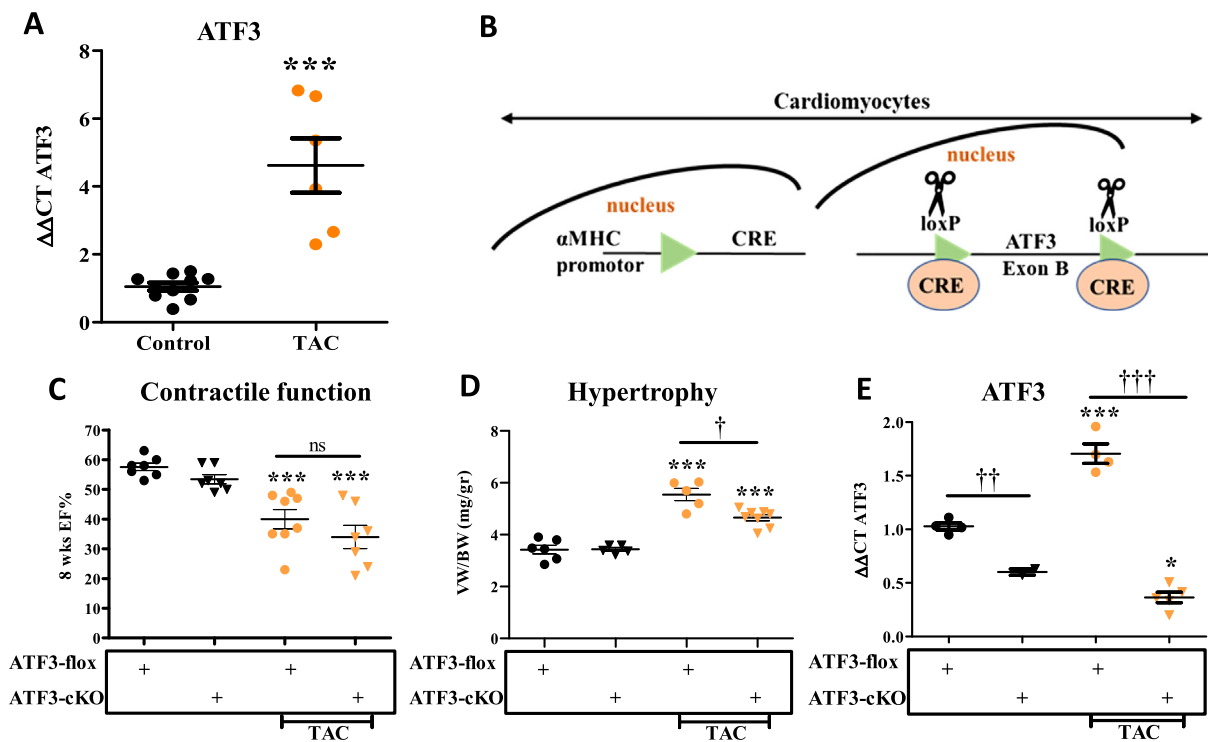


**Fig. 1.** ATF3 expression in cardiomyocytes promotes heart growth following TAC operation. A. mRNA was extracted from ventricles and the expression level of ATF3 was analyzed by qRT-PCR normalized with HSP90 as housekeeping gene. ATF3 transcription at eight weeks following TAC and control. B. Schematic representation for cardiac specific KO.  $\alpha$ MHC-CRE transgenic mouse strain was crossed with ATF3-flox mouse strain (ATF3-flox). CRE is expressed shortly before birth resulting in Exon B excision (loxP sites are indicated) specifically in cardiomyocytes. CRE expressing mice harboring two alleles of ATF3-flox are designated ATF3-cKO. C. Eight weeks following TAC procedure (10–12 weeks old male mice), mice were subjected to MRI. Ejection fraction (EF) was calculated as described in the methods. D. Mice were sacrificed eight weeks following TAC. The hearts were excised and the ventricles weight to body weight ratio is shown (VW/BW). E. mRNA was extracted from ventricles and the expression level of ATF3 was analyzed by qRT-PCR normalized with HSP90 as housekeeping gene.

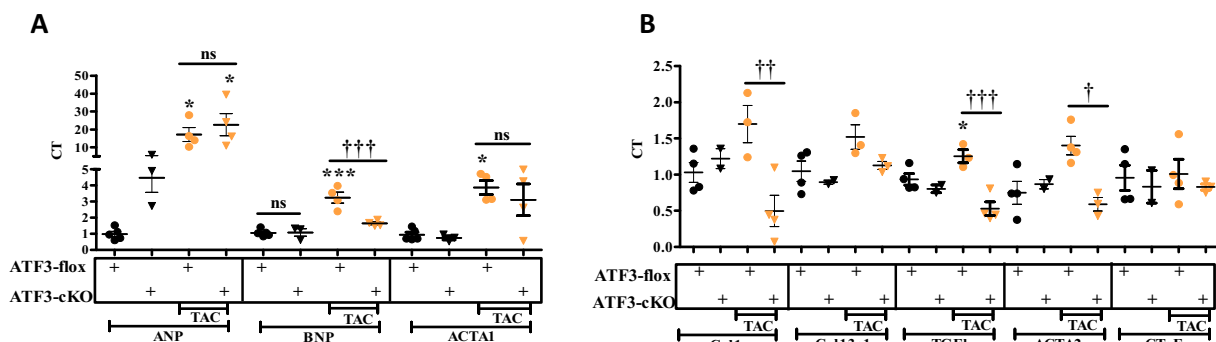


**Fig. 2.** Hypertrophic and Fibrosis gene markers in ATF3-cKO mice. mRNA was extracted from ventricles and the expression levels were measured by qRT-PCR normalized with HSP90 as housekeeping gene. A. Hypertrophic gene markers ANP, BNP and Acta1. B. Fibrosis gene markers Col1 $\alpha$ 1, Col3 $\alpha$ 1, TGF $\beta$ 3, Acta2, CTGF were analyzed. Expression levels are presented as relative values (compared to ATF3-Flox control mice, defined as 1). All results represent the mean  $\pm$  SE \*\*\*  $P \leq 0.05$ , control vs. TAC; † $P \leq 0.05$ , difference between genotypes. Each dot or triangle represents one mouse. n.s. indicates no statistical difference.

scription factors are responsible for altering genetic programs leading to heart failure following multiple chronic stresses. Identification of the key regulators responsible for maladaptive changes may lead to developments of novel approaches and means to prevent heart failure [5,22]. ATF3 is a key regulatory protein found to be elevated in failing hearts [7]. While most of the evidence suggests that ATF3 has a maladaptive role, [9,10,12] others suggested an adaptive role following pressure overload [7], high fat diet [19] and hypertension [23]. In addition, ATF3 over-expression was found to play a cardio-protective role following doxorubicin-induced apoptosis [24]. Nevertheless, gain and loss of function studies have not always led to consistent results and therefore,

the conclusions derived from these studies need to be carefully considered. Genetic ablation of genes is a bona fide tool to study the importance of genes in cardiac remodeling [25]. However, complete gene KO may not necessarily provide conclusive results, since whole animal KO may indirectly lead to adaptive and maladaptive outcomes due to different functional roles in several organs. Moreover, a complex organ such as the heart, which is composed of multiple cell types, may also lead to dichotomous outcome. To better define the role of ATF3 expression in response to pressure overload, a conditional KO approach was used to dissect the role of ATF3 expression in the two main cell types in the heart, fibroblasts and cardiomyocytes. This allowed us to conclude

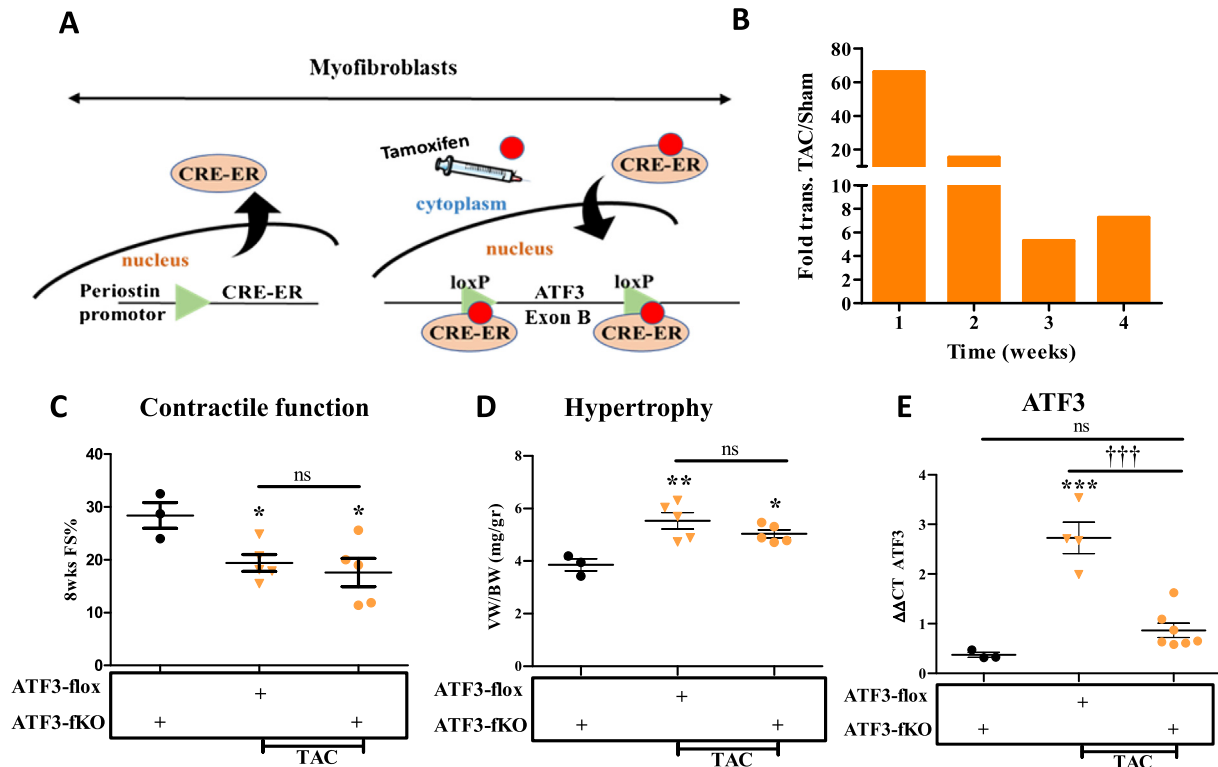


**Fig. 3.** ATF3 expression in myofibroblasts promotes hypertrophic gene program following TAC. A. Schematic representation for fibroblasts specific KO. Periostin-CRE-ER transgenic mouse strain was crossed with ATF3-flox mouse strain (ATF3-flox). CRE-ER is expressed in activated fibroblasts cells. Tamoxifen (red circle) injection is used to facilitate the translocation of CRE-ER into the nucleus resulting in Exon B excision (loxP sites are indicated) specifically in fibroblasts. CRE-ER expressing mice harboring two alleles of ATF3-flox are designated ATF3-fKO. B. RNA-sequencing data analysis for Periostin expression in the hearts of mice at different time points following TAC [16]. C. Eight weeks following TAC (10–12 weeks old male mice), mice were subjected to echocardiography and fractional shortening was calculated as described in the methods. D. Mice were sacrificed eight weeks following TAC. The hearts were excised and the ventricles weight to body weight ratio is shown (VW/BW). E. mRNA was extracted from ventricles and the expression level of ATF3 was analyzed by qRT-PCR. (For interpretation of the references to colour in this figure legend, the reader is referred to the web version of this article.)

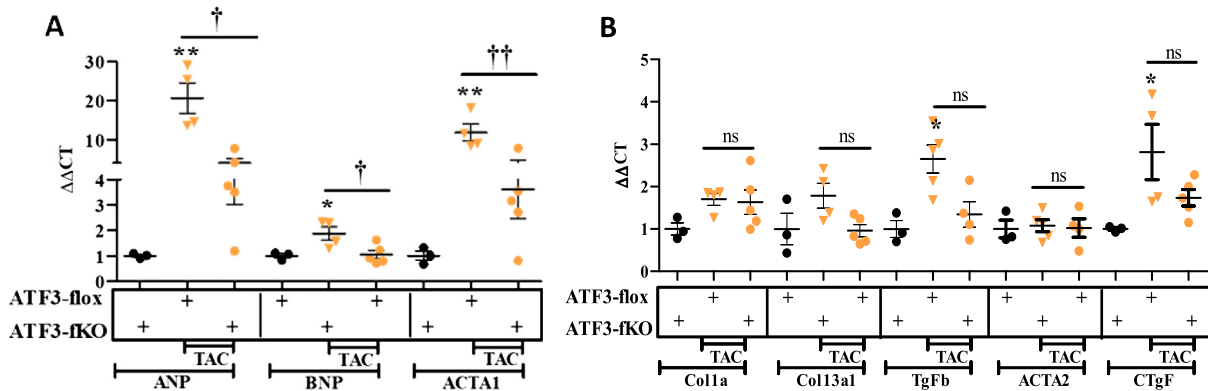


**Fig. 4.** Hypertrophic and Fibrosis gene markers in ATF3-fKO mice. mRNA was extracted from ventricles and the expression level were measured by qRT-PCR. A. Hypertrophic gene markers ANP, BNP and Acta1 B. Fibrosis gene markers Col1 $\alpha$ 1, Col3 $\alpha$ 1, TGF $\beta$ 3, Acta2, CTGF were analyzed. Expression levels are presented as relative values (compared to ATF3-Flox control mice, defined as 1). All results represent the mean  $\pm$  SE \*\*\*  $P < 0.05$ , control vs. TAC; †  $P < 0.05$ , difference between genotypes. Each dot or triangle represents one mouse. n.s. indicates no statistical difference.

that the loss of ATF3 in cardiomyocytes led to a reduced cardiac growth phenotype as compared with the control ATF3-flox control mice following TAC, while hypertrophic markers (ANP and Acta1) and cardiac function were similar. Significantly, although ATF3-cKO displayed reduced VW/BW ratio, this was not accompanied by lower levels of hypertrophic markers. However, we hypothesize that the decreased VW/BW ratio is due to the lower fibrosis levels. In contrast, the loss of ATF3 expression in cardiac fibroblasts displayed a milder hypertrophic hallmark response to TAC as

compared with ATF3-flox control mice, while cardiac function and cardiac growth was similar to control mice. Interestingly, the ablation of ATF3 expression in cardiomyocytes resulted in a significant reduction of fibrosis gene marker response. The cells that express the fibrosis genes are myofibroblasts, and therefore, it is surprising that lack of ATF3 expression in cardiomyocytes resulted in an altered expression of fibrosis genes in the myofibroblasts. Similarly, the ablation of ATF3 expression in myofibroblasts resulted in reduced expression of the hypertrophic gene program.

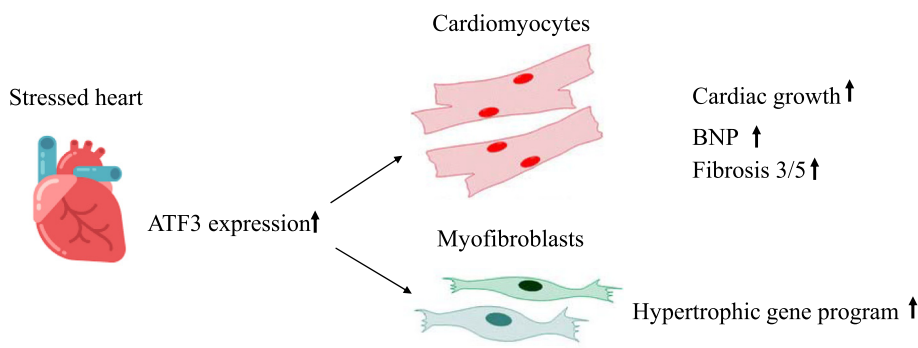


**Fig. 5.** Schematic representation of the main conclusions. Pressure overload stress results in elevation of ATF3 expression in the heart. ATF3 in cardiomyocytes is responsible for cardiac growth and fibrosis gene markers while ATF3 expression in myofibroblasts promotes hypertrophic gene program.

This was unexpected, since cardiomyocytes are the cells in the heart that are responsible for the expression of the hypertrophic genes. We predict that secreted factors, yet to be determined, facilitate the communication between various cell types in the heart. Recent publications show that heart failure promotes tumor growth. Tumor promotion is mediated via the secretion of factors [26] and via recruitment of immune cells [27]. A recent study from our lab, showed that even early stages of cardiac remodeling promote cancer progression and metastasis spread [21]. Thus, it is likely to hypothesize that cardiomyocytes communicate with other cell types in the heart to preserve homeostasis during normal growth as well as following stress. Single cell sequencing analysis may be a method of choice to explore this mode of cooperation between cardiomyocytes and myofibroblasts. Exploring the local as well as distant secreted factors following cardiac stresses may have clinical importance. These can be used to suppress maladaptive cardiac remodeling in the heart and damage to other organs especially for patients with multiple diseases.

In summary, the use of conditional KO mice with differential removal of ATF3 in the two major cardiac resident cells allowed us to dissect the role of ATF3 in these cells. This is consistent with an additive maladaptive effect of ATF3 expression in the remodeled heart.

### 5. Conclusions

ATF3 expression in the heart plays a key role in maladaptive response. While ATF3 expression in cardiomyocytes is mainly responsible for cardiac growth and activation of fibrosis program in myofibroblasts, ATF3 expression in the fibroblasts promotes the hypertrophic gene program in cardiomyocytes (Fig. 5).

### Declaration of Competing Interest

The authors declare that they have no known competing financial interests or personal relationships that could have appeared to influence the work reported in this paper.

### Acknowledgements

We wish to thank the Aronheim lab members for fruitful discussions. The authors thank Prof. Tsonwin Hai from Ohio State University Columbus (USA), for providing ATF3-flox mice.

### Funding

TF was supported by the Rambam-Atidim academic excellence program. This work was supported by the Israel Science Foundation grant # 731/17 to Ami Aronheim.

### References

- [1] J.D. Molkentin, G.W. Dorn 2nd, Cytoplasmic signaling pathways that regulate cardiac hypertrophy, *Annu. Rev. Physiol.* 63 (2001) 391–426.
- [2] Y. Zou, H. Takano, H. Akazawa, T. Nagai, M. Mizukami, I. Komuro, Molecular and cellular mechanisms of mechanical stress-induced cardiac hypertrophy, *Endocr. J.* 49 (2002) 1–13.
- [3] B.C. Bernardo, K.L. Weeks, L. Pretorius, J.R. McMullen, Molecular distinction between physiological and pathological cardiac hypertrophy: experimental findings and therapeutic strategies, *Pharmacol. Ther.* 128 (2010) 191–227.
- [4] J.C. Tardiff, Cardiac hypertrophy: stressing out the heart, *J. Clin. Investig.* 116 (2006) 1467–1470.
- [5] I. Kehat, J.D. Molkentin, Molecular pathways underlying cardiac remodeling during pathophysiological stimulation, *Circulation* 122 (2010) 2727–2735.
- [6] T. Hai, C.C. Wolford, Y.S. Chang, ATF3, a hub of the cellular adaptive-response network, in the pathogenesis of diseases: is modulation of inflammation a unifying component?, *Gene Expr.* 15 (2010) 1–11.
- [7] H. Zhou, D.F. Shen, Z.Y. Bian, J. Zong, W. Deng, Y. Zhang, et al., Activating transcription factor 3 deficiency promotes cardiac hypertrophy, dysfunction, and fibrosis induced by pressure overload, *PLoS ONE* 6 (2011) e26744.
- [8] Y. Okamoto, A. Chaves, J. Chen, R. Kelley, K. Jones, H.G. Weed, et al., Transgenic mice with cardiac-specific expression of activating transcription factor 3, a stress-inducible gene, have conduction abnormalities and contractile dysfunction, *Am. J. Pathol.* 159 (2001) 639–650.
- [9] L. Koren, O. Elhanani, I. Kehat, T. Hai, A. Aronheim, Adult cardiac expression of the activating transcription factor 3, ATF3, promotes ventricular hypertrophy, *PLoS One* 8 (2013) e68396.
- [10] L. Koren, D. Alishekevitz, O. Elhanani, A. Nevelsky, T. Hai, I. Kehat, et al., ATF3-dependent cross-talk between cardiomyocytes and macrophages promotes cardiac maladaptive remodeling, *Int. J. Cardiol.* 198 (2015) 232–240.
- [11] L. Koren, U. Barash, Y. Zohar, N. Karin, A. Aronheim, The cardiac maladaptive ATF3-dependent cross-talk between cardiomyocytes and macrophages is mediated by the IFN $\gamma$ -CXCL10-CXCR3 axis, *Int. J. Cardiol.* 228 (2016) 394–400.
- [12] R. Kalfon, T. Haas, R. Shofti, J.D. Moskovitz, O. Schwartz, E. Suss-Toby, et al., c-Jun dimerization protein 2 (JDP2) deficiency promotes cardiac hypertrophy and dysfunction in response to pressure overload, *Int. J. Cardiol.* 249 (2017) 357–363.
- [13] R. Agah, L.A. Kirshenbaum, M. Abdellatif, L.D. Truong, S. Chakraborty, L.H. Michael, et al., Adenoviral delivery of E2F-1 directs cell cycle reentry and p53-independent apoptosis in postmitotic adult myocardium in vivo, *J. Clin. Investig.* 100 (1997) 2722–2728.
- [14] A.C. deAlmeida, R.J. van Oort, X.H. Wehrens, Transverse aortic constriction in mice, *J. Visual. Exp.: JoVE* (2010).
- [15] R. Kalfon, T. Friedman, S. Eliachar, R. Shofti, T. Haas, L. Koren, et al., JDP2 and ATF3 deficiencies dampen maladaptive cardiac remodeling and preserve cardiac function, *PLoS ONE* 14 (2019) e0213081.
- [16] J.H. Lee, C. Gao, G. Peng, C. Greer, S. Ren, Y. Wang, et al., Analysis of transcriptome complexity through RNA sequencing in normal and failing murine hearts, *Circ. Res.* 109 (2011) 1332–1341.
- [17] C.C. Wolford, S.J. McConoughey, S.P. Jalgaonkar, M. Leon, A.S. Merchant, J.L. Dominick, et al., Transcription factor ATF3 links host adaptive response to breast cancer metastasis, *J. Clin. Investig.* 123 (2013) 2893–2906.

- [18] A. Subramaniam, W.K. Jones, J. Gulick, S. Wert, J. Neumann, J. Robbins, Tissue-specific regulation of the alpha-myosin heavy chain gene promoter in transgenic mice, *J. Biol. Chem.* 266 (1991) 24613–24620.
- [19] R. Kalfon, L. Koren, S. Aviram, O. Schwartz, A. Aronheim, ATF3 expression in cardiomyocytes preserves homeostasis in the heart and controls peripheral glucose tolerances, *Cardiovasc. Res.* 113 (2017) 134–146.
- [20] O. Kanisicak, H. Khalil, M.J. Ivey, J. Karch, B.D. Maliken, R.N. Correll, et al., Genetic lineage tracing defines myofibroblast origin and function in the injured heart, *Nat. Commun.* 7 (2016) 12260.
- [21] S. Avraham, S. Abu-Sharki, R. Shofti, T. Haas, B. Korin, R. Kalfon, et al., Early cardiac remodeling promotes tumor growth and metastasis, *Circulation* 142 (2020) 670–683.
- [22] E. Bisping, P. Wakula, M. Poteser, F.R. Heinzel, Targeting cardiac hypertrophy: toward a causal heart failure therapy, *J. Cardiovasc. Pharmacol.* 64 (2014) 293–305.
- [23] Y. Li, Z. Li, C. Zhang, P. Li, Y. Wu, C. Wang, et al., Cardiac fibroblast-specific activating transcription factor 3 protects against heart failure by suppressing MAP2K3-p38 signaling, *Circulation* 135 (2017) 2041–2057.
- [24] K. Nobori, H. Ito, M. Tamamori-Adachi, S. Adachi, Y. Ono, J. Kawauchi, et al., ATF3 inhibits doxorubicin-induced apoptosis in cardiac myocytes: a novel cardioprotective role of ATF3, *J. Mol. Cell. Cardiol.* 34 (2002) 1387–1397.
- [25] J. Davis, M. Maillet, J.M. Miano, J.D. Molkentin, Lost in transgenesis: a user's guide for genetically manipulating the mouse in cardiac research, *Circ. Res.* 111 (2012) 761–777.
- [26] W.C. Meijers, M. Maglione, S.J.L. Bakker, R. Oberhuber, L.M. Kieneker, S. de Jong, et al., Heart failure stimulates tumor growth by circulating factors, *Circulation* 138 (2018) 678–691.
- [27] G.J. Koelwyn, A.A.C. Newman, M.S. Afonso, C. van Solingen, E.M. Corr, E.J. Brown, et al., Myocardial infarction accelerates breast cancer via innate immune reprogramming, *Nat. Med.* 26 (2020) 1452–1458.